

Investigation of Parallel Heat-flow Path in Electro-thermal Microsystems

Péter G. Szabó, Vladimír Székely

Budapest University of Technology and Economics (BME)

Department of Electron Devices

szabop | szekely@eet.bme.hu

Abstract- Due to the miniaturization seen in the last decades, several macro models that neglect parameters have to be revised in order to evaluate the behavior of different types of microsystems. In this paper we present the analysis of one such parameter which affects the thermal functionality, namely, the convection of natural gases. In macro scale this parameter is usually neglected, because the conductivity of gases is several magnitude smaller than that of the base materials. With the advance of microfabrication really good thermal isolation can be achieved and so their values can be evenly compared and the models have to be revised. This effect can be easily modeled on microstructures whose thermal resistance can be compared to the thermal conductivity of natural gases and whose output is temperature dependent. For this purpose different types of cantilevers with embedded thermopiles and heating resistors were used. The modeling and experimental results show that in microsystems that are sensitive to temperature change, the parallel heat flow created by the surrounding gases have significant impact on the operation.

I. INTRODUCTION

In the field of microdevices several group of microsystem are working in the electro-thermal domain. Nowadays several actuator and sensor applications are being developed where the parameters of the thermally stimulated structure change, resulting in an observable effect. An example for this issue comes up, if electronically generated thermal energy is being converted back to electricity based on the Seebeck effect. Utilizing this principle, special microsystems can be developed with several functions.

In order to better understand the operation of these systems and to obtain optimal designs, the precise characterization of these structures is essential. As for micro-scale sizes the well known behavior of macro objects can not be strictly interpreted to micro objects. With the result of scaling in size, MEMS devices provide - for example - much stronger electrostatic forces compared to electromagnetic forces which explains why micromachines with electrostatic moving principle of operation are much more widespread than their electromagnetically actuated counterparts.

A similar issue can be observed at electro-thermal microsystems. In macro objects the thermal conductance of air is so small compared to other materials that it is usually neglected and only its convection is calculated in the system description. However in microsystems where really good thermal isolation can be realized, the conductance of thin air

layer that surrounds the structure is comparable to the thermal conductance of the structural materials. This means that additional analysis is needed especially in those systems where the efficiency highly depends on good isolation. One method to calculate with parasitic heat flow was presented in [1] where the effect of the parallel heat flow path has been considered with a single parallel thermal resistance. The paper also presented thermal transient measurements where the differences between normal atmospheric and vacuum conditions were observed.

In this paper we present our results of studying the effects of the parallel heat flow path, which is created in electro-thermal microstructures by the surrounding air. The analysis is verified on a Quadratic Transfer Characteristics (QTC) microelement which is introduced in [2] and we have already analyzed its operation in [3][4]. In section 2 we recap the basic principles of the QTC element. In the third section we discuss how the parallel flow comes into sight, how and what rate it effects the previously set statements, system descriptions [4]. As an outcome we also make model revisions to improve our preceding models. The theory will be verified in the fourth and fifth sections. The fourth chapter provides data on the steady state measurements with a few explanations about the measurement methods. In the fifth chapter the transient behavior is investigated whereof we can draw our conclusion regarding our examination.

II. BASICS OF THE QTC ELEMENT

The basic structure is shown in Figure 1. A dissipating resistance (R) heats up a region H of the substrate while a thermocouple array senses the temperature difference between the H hot region and the C cold side. Since the dissipated heat is related to the square of the V_{in} voltage, the T_H-T_C temperature difference and thus the output voltage will be proportional to the square of V_{in} .

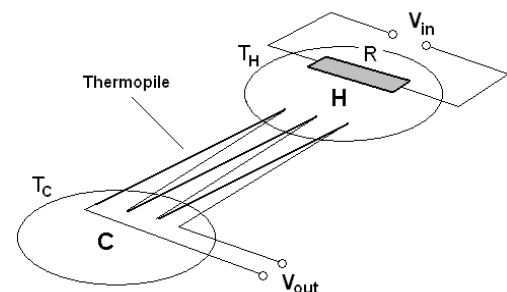


Figure 1 Principle of the QTC element

The DC transfer characteristics of the structure can be calculated as follows. The dissipated heat flux is

$$P_J = V_{in} \cdot I = V_{in}^2 / R \quad (1)$$

The temperature rise of the H hot region with respect to the cold region is

$$T_H - T_C = P_J \cdot R_{th} \quad (2)$$

where R_{th} is the thermal resistance (K/W) between regions H and C . Finally the output voltage is

$$V_{out} = N \cdot S \cdot (T_H - T_C) = N \cdot S \cdot R_{th} \cdot V_{in}^2 / R \quad (3)$$

where S is the Seebeck constant for the material pair of the thermocouples, N is the number of the serially connected thermocouples.

It is obvious that the structure realizes quadratic voltage transfer characteristics:

$$V_{out} = K \cdot V_{in}^2 \quad (4)$$

where K is the conversion constant of the device:

$$K = \frac{N \cdot S \cdot R_{th}}{R} \quad (5)$$

In order to construct a useful device K has to be reasonably large. Because of the need for a large value of R_{th} , the early monolithic realizations [2] were less successful, due to the small thermal resistance appearing between the two regions of silicon bulk. The situation changed dramatically with the advance of the era of microsystems. By using cantilevers or bridges made of e.g. SiO_2 the thermal resistance between the hot and cold regions can be increased by orders of magnitude.

For the experiments we use a chip from TIMA Laboratory [5]. On this chip the thermal functional elements were fabricated by a combination of bulk micromachining and CMOS technology. Four of the previously described circuits were realized on cantilevers, which trail over an etched cavity. One of these structures is shown in Figure 2.

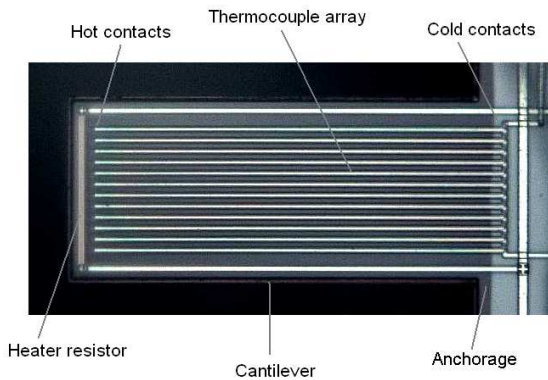


Figure 2 The QTC microsystem

The cantilevers, of dimensions $210 \times 100 \mu\text{m}^2$, are made basically of SiO_2 with buried poly-Si and Al strips. The thickness of the cantilever is $4.23 \mu\text{m}$. The heater resistor is $3 \mu\text{m}$ wide and $86 \mu\text{m}$ long. The hot points of the thermopiles are placed at $4.3 \mu\text{m}$ right of the heater resistor. 12 pieces of poly-silicon/aluminum thermocouples were fabricated with $1.4 \mu\text{m}$ width and $213.8 \mu\text{m}$ length.

The other three structures are different to some extent.

There is one other $210 \mu\text{m}$ long cantilever with two heater resistors (R_1 and R_2) parallel placed in the H point and there are two other cantilevers with $100 \mu\text{m}$ length - instead of $210 \mu\text{m}$ - where one of the structures has two heater resistors (R_1 and R_2) while the other one has only one (R).

III. EFFECTS OF THE PARALLEL HEAT FLOW

A well known method in the field of thermodynamics, heat transfer etc. [6][7] is to use thermal equivalent circuits when the thermal behavior of a system is being described. Basically this technique is used to simplify the description of the system in a compact form where the numerical analysis becomes easier. However, depending on the size and the shape of the various structures being analyzed, it is usually not a straightforward task to give a precise circuit that describes the system correctly. When a simple system is investigated its heat flow path can be described with thermal R-C ladders. So in the first steps, for the sake of simplicity let us cope with a 2 stage Cauer R-C ladder.

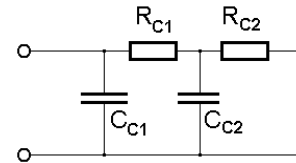


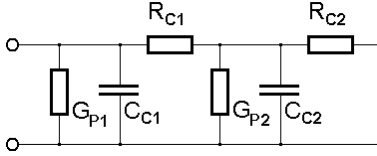
Figure 3 Cauer R-C ladder

This circuit which is presented in Figure 3, represents one dimensional heat conduction along the cantilevers where all the secondary paths are ignored. If the air which surrounds the system is taken into consideration then it can be represented by a heat conductance, a heat capacitance connected parallel to the ladder.

Let us examine the parameters of this secondary path. In simple systems usually one may assume natural convection, i.e. $h_{air} = 5-10 \text{ W/m}^2\text{K}$ heat transfer coefficient can be used. If we assume that this coefficient is not changing with the scaling, then for a typical microsystem whose area is in the range of hundreds μm^2 , this power lost to dissipation is in the range of 10^{-5} W , that is about a few percent compared to the power generated by the resistor.

Furthermore the thermal capacitance of the surrounding air can still be considered negligible compared to that of the structure. At the same time the calculation of thermal conductance shows different results. If the cantilever with $l=210 \mu\text{m}$ length and $w=100 \mu\text{m}$ width is taken into consideration the estimated thermal resistance of the air between the cantilever and the bottom of the cavity is in the range of 10^4-10^5 K/W . This rough estimation can be compared to the heat resistance of the QTC MEMS in [4] that is $7.2 \cdot 10^4 \text{ K/W}$, which fact motivates our investigations in this field.

It can be stated that only the thermal conductance parameter of the air is significant enough to be used in the equivalent circuit which is presented in Figure 4. It is worth considering calculating with the convection because of the few percent heat loss it causes. It can be modeled as an additional small conductance that is included in the heat conductance of the air.


Figure 4 Cauer R-C ladder with parallel conductances (G_p)

Based on Figure 4 it is evident that the temperature of a properly thermally insulated microsystem can be reduced remarkably when it is surrounded by air and not by vacuum. As it can be noticed that in steady state it is possible that the maximum temperature can even be dropped by 40 % compared to the temperature in vacuum.

Nevertheless this conductance alters the time dependent behavior as well. As written in [8] without considering the parallel heat flow, the thermal transfer impedance between the substrate side and the end of the cantilever can be calculated as

$$Z_{th}(s) = \frac{R_{th}}{\sqrt{s \cdot R_{th} \cdot C_{th}}} \cdot \tanh(\sqrt{s \cdot R_{th} \cdot C_{th}}) \quad (6)$$

where R_{th} is the thermal resistance, C_{th} is the thermal capacitance and s is the complex frequency. This impedance function has poles in an infinite number lying on the negative real axis that can be determined as:

$$|\sigma| = \frac{1}{\tau} = (2 \cdot n + 1)^2 \cdot \frac{\pi^2}{4 \cdot R_{th} \cdot C_{th}} \quad n = 0 \dots \infty \quad (7)$$

with their corresponding magnitudes:

$$R_p = \text{Re } s / |\sigma| = \frac{8 \cdot R_{th}}{(2 \cdot n + 1)^2 \cdot \pi^2} \quad (8)$$

However when the structure is not in vacuum, the G_{th} parallel conductance has to be taken into account in the thermal transfer impedance

$$Z_{th}(s) = \frac{R_{th}}{\sqrt{R_{th} \cdot (s \cdot C_{th} + G_{th})}} \cdot \tanh(\sqrt{R_{th} \cdot (s \cdot C_{th} + G_{th})}) \quad (9)$$

which results in a change in the location of the poles

$$|\sigma| = \frac{1}{\tau} = (2 \cdot n + 1)^2 \cdot \frac{\pi^2}{4 \cdot R_{th} \cdot C_{th}} + \frac{G_{th}}{C_{th}} \quad (10)$$

with a decrease in the corresponding magnitudes:

$$R_p = \text{Re } s / |\sigma| = \frac{2 \cdot R_{th}}{(2 \cdot n + 1)^2 \cdot \frac{\pi^2}{4} + R_{th} \cdot G_{th}} \quad (11)$$

IV. STEADY STATE MEASUREMENTS

A. Measurement setup

To verify our theory, preliminary measurements have to be made which also reveal the robustness of the effect. Hence the package which contains the microsystems bound to a small PCB was placed into vacuum chamber. With the ability of in-situ measurement we can measure the structure under three different pressure conditions:

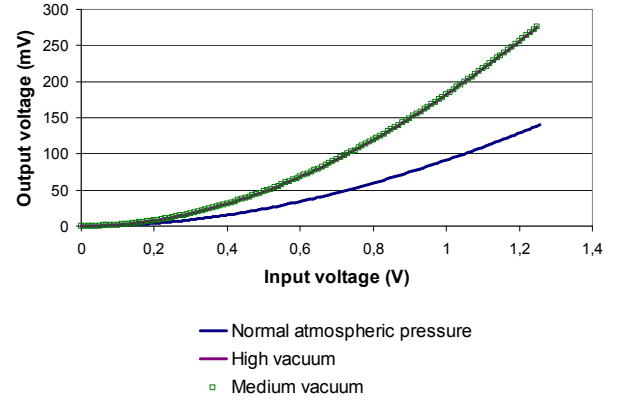
- normal atmospheric pressure which is around 101.3 kPa in 100 m above sea level at 47° north.

- medium vacuum state which is between 6.66-2.66 Pa.
- high vacuum state which below 3.8 mPa.

B. Input-output characteristics

Using the previously described setup, we measured how the input-output characteristics differs from those we measured under normal atmospheric conditions.

Figure 5 shows the characteristics of the 210x100 μm^2 cantilever with one heating resistor under all three pressure condition.


Figure 5 I/O characteristics of 210x100 μm^2 cantilever

By using polynomial approximation, the fourth order approximation functions of the cantilever become:

$$V_{\text{out atm}} = (-2.13 \cdot V_{in}^4 - 5.85 \cdot V_{in}^3 + 99.87 \cdot V_{in}^2 - 0.45 \cdot V_{in} + 0.023) \cdot 10^{-3}$$

$$V_{\text{out mv}} = (-3.99 \cdot V_{in}^4 - 13.49 \cdot V_{in}^3 + 200.64 \cdot V_{in}^2 - 1.1 \cdot V_{in} + 0.05) \cdot 10^{-3}$$

$$V_{\text{out hv}} = (-4.1 \cdot V_{in}^4 - 13.36 \cdot V_{in}^3 + 200.64 \cdot V_{in}^2 - 1.08 \cdot V_{in} + 0.04) \cdot 10^{-3} \quad (12)$$

The equations and the figure clearly point out the correlation between the pressure conditions in the surroundings. It was also evident that differences between medium and high vacuum stages are minimal which is obvious if we calculate the mean free path between the molecules using [9][10]:

$$l = \frac{k_B \cdot T}{\sqrt{2} \cdot \pi \cdot 4 \cdot r^2 \cdot p} \quad (13)$$

where $k_B = 1.38 \cdot 10^{-23} \text{ J} \cdot \text{K}^{-1}$ is the Boltzmann constant, T is the temperature which is in the range of 293-478 K, $r = 0.186 \text{ nm}$ is the mean radius of the air molecules [10] and p is the pressure. These conditions result in 982-4016 μm mean free path in medium vacuum and 1.72-2.81 m in high vacuum.

As not only the cantilever shown in Figure 5 was measured, Table I presents the approximation functions of the other QTC elements¹ and the output voltage when the

¹As stated in section III. there are 4 types of cantilevers, two with 210 μm and two with 110 μm length. Ones of these two cantilevers have one heating resistor (R) and the other ones have two (R1 and R2), where R2 is closer to the thermopiles and R1 is farther.

systems are excited by 1.25 V.

D. Resistance measurements and temperature calculations

TABLE I

STEADY STATE OUTPUT VOLTAGE VALUES OF THE MICROSYSTEMS

	Heater resistor	Output voltage		V ² term of the approximation function x10 ⁻³	
		at 1 ATM	below 3.8 mPa	at 1 ATM	below 3.8 mPa
210 μm long cantilevers	R1	119 mV	221 mV	78.04	148.9
	R2	128 mV	247 mV	83.54	164.72
	R	140 mV	276 mV	99.87	200.64
110 μm long cantilevers	R1	82 mV	106 mV	52.18	71.39
	R2	88 mV	122 mV	55.66	79.84
	R	98 mV	140 mV	62.34	92.81

C. Rise in the Peltier effect induced voltage

As presented in [4] if the heating resistor is in operation it generates asymmetrical temperature distribution as a result of the Peltier-effect which is due to the aluminum-polysilicon contacts at the ends of the resistor. This asymmetry can be measured with the help of the microsystems with two heating resistors. By switching on voltage to one of the resistors, the generated temperature distribution induces Seebeck-effect on the ends of the undriven resistor.

Figure 6 shows this induced voltage compared to the input voltage on the 210x100 μm² cantilever when it is heated by the R1 resistor.

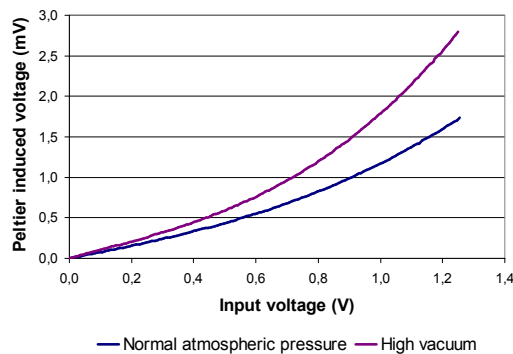


Figure 6 Peltier induced voltage on the 210x100 μm² cantilever

As in the previous section Table II presents the measurement results on the other cantilever.

TABLE II

PELTIER EFFECT INDUCED OUTPUT VOLTAGE VALUES

	Heater resistor	Output voltage	
		at 1 ATM	below 3.8 mPa
210 μm long cantilevers	R1	~1.57 mV	~2.8 mV
	R2	~0.8 mV	~1.43 mV
110 μm long cantilevers	R1	~1.43 mV	~2 mV
	R2	~0.74 mV	~1.14 mV

The microsystems with two heating resistors can be used not just to investigate the Peltier-effect, but to give a good approximation of the temperature in the hottest points of the structures. In order to do so one of the heating resistors has to be used as a bolometer while the other resistor is heated. However to find out the temperature dependent parameters of the bolometer, the increase of its resistance has to be recorded against the temperature increase.

Furthermore, when setting up the resistance measurement special attention must be paid because conventional resistance measurements push significant amount of current through the resistors [11], heating the system itself, and producing inaccurate results. To eliminate the unwanted heating, a voltage divider based voltage measurement setup was used.

However by using this setup, different characteristics are obtained when the polarity of the heater resistor is inverted. This is because of the Peltier effect induced voltage. It can be represented by an additional voltage generator connected in series with the bolometer. When the polarity of the heating voltage is reversed it results in an axis-mirrored temperature distribution map, which also inverts the polarity of the represented voltage generators that shifts the measured characteristics. To compensate it, the Peltier effect induced voltage characteristics have to be subtracted from the scaled voltage characteristics and then it can be converted to resistance function.

TABLE III

INCREASES OF THE RESISTANCES AND THE MAXIMUM TEMPERATURES

	Heater resistor	ΔR on the heated resistor		Temperature	
		at 1 ATM	below 3.8 mPa	at 1 ATM	below 3.8 mPa
210 μm long cantilevers	R1	54.4 Ω	100 Ω	110 °C	185 °C
	R2	67.7 Ω	122.4 Ω	125 °C	200 °C
110 μm long cantilevers	R1	43.2 Ω	61.2 Ω	100 °C	130 °C
	R2	48 Ω	79 Ω	105 °C	150 °C

In Table III the results of this measurement process are presented when the structures are excited by 1.25 V. It must be mentioned that despite the fact that we are not able to measure the temperature of the cantilevers with one heating resistor we can still provide a good approximation of their maximum temperature based on the calculated material properties in [4]. In Table III the temperatures generated by 1.25 V are also presented. These values are derived from the resistance-temperature measurement where the structure is placed into a thermostat, and the scaled voltages – see Figure 7 - are measured in the range of 5-100 °C. As the resistance-temperature characteristics have a quasi-constant temperature dependent coefficient, the values above 100 °C are approximated with the mean value of the temperature dependent constants.

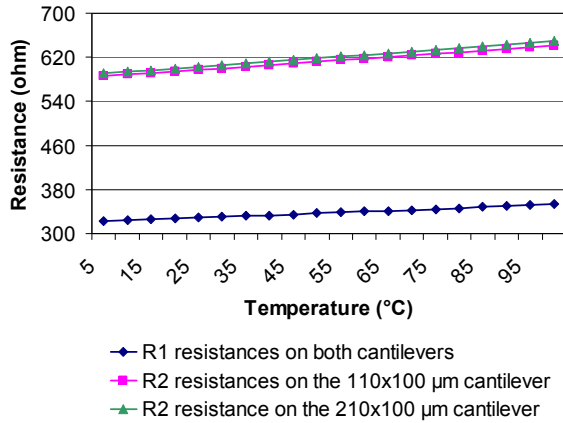


Figure 7 Resistance vs. Temperature

V. TRANSIENT MEASUREMENTS

According to [12] transient measurement can be used to reveal the thermal properties of a structure. Since, if a circuit is driven by a step voltage input, its response function shows the thermal and electrical properties of the system. By using appropriate setup, the electrical capacitances and loads can be filtered and the thermal parameters can be calculated from the residual function as presented in [13].

Based on these considerations we used a thermal transient tester to measure the transient response of the microsystems. To achieve appropriate signal levels (i.e. to perform impedance matching) an amplifier with unit gain and noise suppression is placed between the structure and the tester. In addition, to avoid burn out which is caused by accidental overload, a current divider circuit is connected between the tester driver output and the input of the microsystem. This circuit together with the measurement setup can be seen in Figure 8.

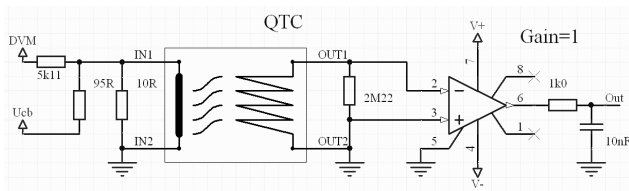
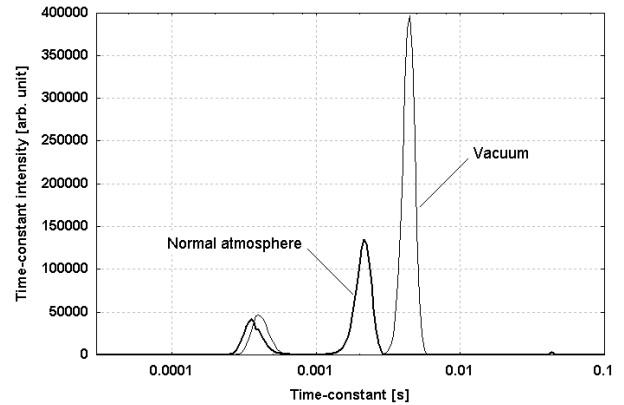


Figure 8 Transient measurement setup

To validate our model we need to examine the time constants of the structures which can be read from Tau-intensity function [6].

Figure 9 shows these tau-intensity functions of the 210x100 μm² cantilever with one heating resistor. The thick curve belongs to 1 ATM pressure and the thin curve to the medium vacuum state.


 Figure 9 Tau-Intensity function of the 210x100 μm² cantilever with one heating resistor

It is clearly visible that the magnitude and the location of the first and second time constants have changed. Table IV presents the decreased intensities as percentage of their initial values and the locations of the first time constants of the cantilevers.

TABLE IV

MEASURED TIME CONSTANTS AND THE DECREASED INTENSITY VALUES

	Heater resistor	Time constant		Decreased intensity values
		at 1 ATM	below 6 Pa	
210 μm long cantilevers	R2	2.15 ms	4.14 ms	44.5 %
	R	2.15 ms	4.47 ms	42.0 %
110 μm long cantilevers	R1	0.89 ms	1.21 ms	68.9 %
	R	0.96 ms	1.36 ms	64.7 %

According to Table IV the thermal resistance of the gas surrounding the cantilevers can be approximated by using (7)(10).

$$G_{th} = \left(\frac{1}{\tau_{atm}} - \frac{1}{\tau_{vac}} \right) \cdot C_{th} \quad (14)$$

where C_{th} is calculated using [4][14][15]. The results for each structure are presented in Table V.

TABLE V

APPR. THERMAL RESISTANCES OF THE AIR

	Heater resistor	Appr. thermal resistance of the air
210 μm long cantilevers	R2	3·10 ⁴ K/W
	R	2.79·10 ⁴ K/W
110 μm long cantilevers	R1	4.32·10 ⁴ K/W
	R	4.19·10 ⁴ K/W

These results points out our expectations that the smaller cantilevers have less air surrounding, which means their parallel conductance is smaller.

The value of the G_{th} parallel heat loss can be determined

by using the measurement data for static characteristics. Observing Figure 5 we can state that the sensitivity at normal atmospheric pressure is 50% of the value measured in vacuum chamber (case of 210 μm long structure). This is caused by the decrease of R_{th} value in (5). This decrease can be followed by using (9) for the steady-state ($s = 0$) case:

$$R_{th}^* = Z_{th0} = \sqrt{\frac{R_{th}}{G_{th}}} \tanh(\sqrt{R_{th}G_{th}}) \quad (15)$$

The plot of this function is shown in Figure 10. The 50% decay in R_{th} gives 37500 K/W. The corresponding G_{th} value is $4.78 \cdot 10^{-5}$ W/K.

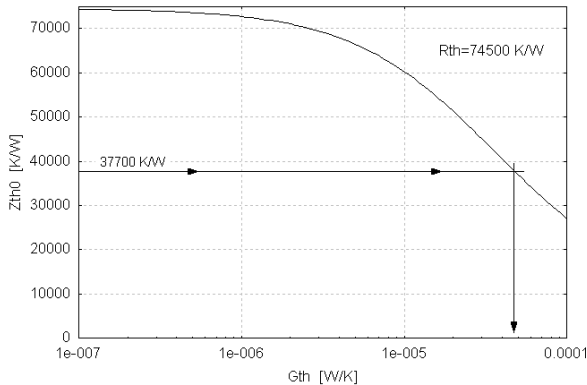


Figure 10 Plot of (15)

We can also verify our theory by comparing the results of Table IV against the analytical results - presented in Table VI - given by substituting the thermal conductivity of air into (7) (8) (10) (11) and using the layout and material data from [3][4][14][15][16]. In the calculations the thermal conductance of air was approximated by calculating the thermal conductance of the cavity under the cantilever where we assumed that the heat spreading is not strictly rectangular.

TABLE VI

CALCULATED TIME CONSTANTS AND THE DECREASED INTENSITY VALUES

	Heater resistor	Time constant		Decreased intensity values
		Using (10)	Using (7)	
210 μm long cantilevers	R2	2.51 ms	4.06 ms	61.9 %
	R	2.68 ms	4.48 ms	59.9 %
110 μm long cantilevers	R1	0.91 ms	1.15 ms	79.2 %
	R	0.96 ms	1.23 ms	78.1 %

It can be seen that the results are in the same order of magnitude. The differences may be originated from the different material properties and from the rough estimation of the heat conductance of the air ($\lambda_{\text{Air}}=0.026$ W/mK) that surrounds the cantilever.

VI. CONCLUSION

The presented case study shows an investigation of how the gaseous environment around an electro-thermal microsystem can decrease the effectiveness. The idea is based on the fact that the heat conduction of the surrounding

air is usually neglected, because its conductance is at least ten times smaller than the materials of the structure. But, when the main operation area is well isolated from the main heat spreader body from a thermal point of view the conductance of the gas can be evenly compared and should not be neglected. Our experiments show that the efficiency of an electro-thermal MEMS can be dropped down to nearly 50 % compared to the values measured in vacuum.

ACKNOWLEDGMENT

The authors acknowledge the help and contribution of their colleagues, especially S. Török for the construction of the PCB board used in the transient measurements and L. Juhász for the assistance in the vacuum measurements. The present research is partly funded by the National Office for Research and Technology (contract ID: OMFB-00521/2009) and the ENIAC of the EU through the SE2A project.

REFERENCES

- [1] M. Rencz, A. Poppe, E. Kollár, S. Rész, V. Székely, "Increasing the accuracy of structure function based thermal material parameter measurements", *IEEE Transactions on components and packaging technologies*, Vol. 28, No. 1 pp. 51-57. 2005
- [2] V. Székely, "New type of thermal-function IC: The 4-quadrant multiplier", *Electronics Letters*, Vol. 12, No. 15, pp. 372-373., 22nd July 1976
- [3] P. G. Szabó, V. Székely, "Characterization and Modeling of an Electro-thermal MEMS Structure", *Collection of Papers Presented at the DTIP of MEMS & MOEMS 2008*, 9-11 April 2008
- [4] P. G. Szabó, V. Székely, "Characterization and modeling of electro-thermal MEMS structures" *MICROSYSTEM TECHNOLOGIES*, Vol. 15. No. 8, pp. 1293-1301. August, 2009
- [5] B. Charlot, S. Mir, E. F. Cota, M. Lubaszewski, B. Courtois, "Fault simulation of MEMS using HDLS" *Proceedings of SPIE*, Vol. 3680, pp. 70-77. 1999
- [6] V. Székely, Tran Van Bien, "Fine structure of heat flow path in semiconductor devices: a measurement and identification method" *Solid-State Electronics* Vol. 31, No. 9, pp. 1363-1368. February 1988
- [7] V. Székely, "On the representation of infinite-length distributed RC one-ports", *IEEE Trans. on Circuits and Systems*, Vol.38. pp. 711-719, 1991
- [8] V. Székely, "THERMODEL: A tool for compact dynamic thermal model generation", *Microelectronics Journal* Vol. 29, pp. 257-267., 1998
- [9] J. O. Hirschfelder, C. F. Curtiss, R. B. Bird, "Molecular theory of gases and liquids", *John Wiley & Sons, Inc.*, 1954
- [10] A. Budó, "Kísérleti fizika I." in hungarian, "Experimental physics", *Nemzeti Tankönyvkiadó CPLC.*, 2004
- [11] "Agilent 34401A Multimeter - Uncompromising Performance for Benchtop and System Testing - Product Overview", *Agilent Technologies*, 2007
- [12] B. Smith, T. Brunschwiler, B. Michel, "Comparison of transient and static test methods for chip-to-sink thermal interface characterization", *Microelectronics Journal*, Vol. 40, pp. 1379-1386, 2009
- [13] V. Székely, M. Rencz, B. Courtois, "Thermal Transient Testing", *Microelectronics International*, Vol. 14, No. 2, pp. 8-10. 1997 DOI: 10.1108/13565369710800529
- [14] Y. S. Ju and K. E. Goodson, "Process-dependent thermal transport properties of silicon-dioxide films deposited using low-pressure chemical vapor deposition", *Journal of Applied Physics*, Vol. 85, No. 10, May 1999
- [15] F. P. Incropera, D. P. De Witt, "Introduction to heat transfer", *John Wiley & Sons*, Second edition, 1985
- [16] M. von Arx, O. Paul, H. Baltes, "Process-dependent thin-film thermal conductivities for thermal CMOS MEMS", *IEEE Journal of Microelectromechanical Systems*, Vol. 9, No. 1, pp. 136-145, March 2000